ANTIMICROBIAL AGENTS AND CHEMOTHERAPY, Feb. 2008, p. 694–704 Vol. 52, No. 2
0066-4804/08/$08.00+0 doi:10.1128/AAC.00861-07

Multidrug Transporters CaCdr1p and CaMdr1p of *Candida albicans* Display Different Lipid Specificities: both Ergosterol and Sphingolipids Are Essential for Targeting of CaCdr1p to Membrane Rafts▽

Ritu Pasrija,[1]† Sneh Lata Panwar,[2] and Rajendra Prasad[1]*

Membrane Biology[1] and Yeast Genetics[2] Laboratories, School of Life Sciences, Jawaharlal Nehru University, New Delhi 110067, India

Received 2 July 2007/Returned for modification 10 September 2007/Accepted 16 November 2007

In this study, we compared the effects of altered membrane lipid composition on the localization of two membrane drug transporters from different superfamilies of the pathogenic yeast *Candida albicans*. We demonstrated that in comparison to the major facilitator superfamily multidrug transporter CaMdr1p, ATP-binding cassette transporter CaCdr1p of *C. albicans* is preferentially localized within detergent-resistant membrane (DRM) microdomains called 'rafts.' Both CaCdr1p and CaMdr1p were overexpressed as green fluorescent protein (GFP)-tagged proteins in a heterologous host *Saccharomyces cerevisiae*, wherein either sphingolipid (Δ*sur4* or Δ*fen1* or Δ*ipt1*) or ergosterol (Δ*erg24* or Δ*erg6* or Δ*erg4*) biosynthesis was compromised. CaCdr1p-GFP, when expressed in the above mutant backgrounds, was not correctly targeted to plasma membranes (PM), which also resulted in severely impaired drug resistance. In contrast, CaMdr1p-GFP displayed no sorting defect in the mutant background and remained properly surface localized and displayed no change in drug resistance. Our data clearly show that CaCdr1p is selectively recruited, over CaMdr1p, to the DRM microdomains of the yeast PM and that any imbalance in the raft lipid constituents results in missorting of CaCdr1p.

In pathogenic as well as nonpathogenic yeasts, several mechanisms can contribute to the development of multidrug resistance (MDR). Point mutations or overexpression of the drug target, a decrease in the import of drugs, and an enhanced efflux of drugs are some of the strategies employed by drug-resistant yeast to overcome the lethal effects of the drugs (4, 8, 39, 40). However, extrusion of noxious compounds from the cell, mediated by efflux pumps, is one of the most frequently used strategies for the development of drug resistance in yeasts, which holds true for several prokaryotic and eukaryotic organisms (38, 41, 48).

The two major efflux pump proteins involved in MDR belong to ATP-binding cassette (ABC) and major facilitator (MFS) superfamilies. Genome analysis of *Saccharomyces cerevisiae* and of the pathogenic yeast *Candida albicans* reveal the existence of 30 and 28 putative ABC transporters, respectively, of which only a few function as drug transporters (9, 17). Similar to the ABC protein superfamily, very few members of the MFS family are drug exporters. For example, out of 62 putative transporters in *S. cerevisiae* (6), only *FLR1* (fluconazole resistance) has been shown to confer resistance to drugs (7). In pathogenic *C. albican*s, out of 71 MFS proteins, only Ca*MDR1* is known to extrude drugs, where its overexpression has been linked to azole resistance (6, 35).

The efflux pumps CaCdr1p and CaMdr1p are both localized on the plasma membrane (PM) (35, 43). Interestingly, CaCdr1p is sensitive to changes in the membrane environment and also plays a role in maintaining membrane asymmetry (24, 32, 34, 37, 44). Human Pgp/*MDR1*, a homologue of the yeast ABC proteins, is predominantly localized in microdomains within the PM. The presence of the microdomains, also called 'lipid rafts,' in various organisms plays an important role in cell signaling, protein sorting, and virulence (13, 29, 30, 31, 36, 47). Lipid rafts are highly enriched in sphingolipid and ergosterol or cholesterol and are characterized by their insolubility in detergent (1, 2, 15, 22). Depletion of cholesterol from these domains impairs Pgp-mediated drug transport in a substrate- and cell-type-specific manner (11). It is also observed that human Pgp/*MDR1* contributes to stabilize the cholesterol-rich microdomains by mediating cholesterol redistribution within the cell membrane (16). The acquisition of the MDR phenotype in certain mammalian cell lines is not only due to overexpression of the drug efflux pumps but is also accompanied by an upregulation of genes required for normal lipid metabolism that constitute membrane rafts (26). In yeasts as well, we have previously shown that efflux pump proteins, particularly of the ABC superfamily, are influenced by imbalances in membrane lipid composition (32, 34, 37, 44). The presence of detergent-resistant membranes (DRMs) within the yeast PM has recently been demonstrated (29, 46). In order to critically evaluate the role of the DRM lipid constituents in the localization of the efflux pumps, in this study, we have overexpressed green fluorescent protein (GFP)-tagged CaCdr1p and CaMdr1p in different lipid mutant backgrounds of *S. cerevisiae*. The mutants used were defective either in the ergosterol (Δ*erg24* or Δ*erg6* or Δ*erg4*) or in the sphingolipid (Δ*sur4* or Δ*fen1* or Δ*ipt1*) biosynthesis pathway.

Here we report that the observed abrogated functioning of

* Corresponding author. Mailing address: Jawaharlal Nehru University, School of Life Sciences, JNU Campus, New Mehrauli Road, New Delhi 110067, India. Phone: 91-11-2670-4509. Fax: 91-11-2674-1081. E-mail: rp47@mail.jnu.ac.in.

† Present address: Department of Molecular Biology and Biochemistry, Guru Nanak Dev University, Amritsar, India.

▽ Published ahead of print on 3 December 2007.

TABLE 1. List of yeast strains used in this study

Strain	Genotype	Source or reference
AD1–8u$^-$	Mat**a** *pdr1-3 his1 ura3 Δyor1::hisG Δsnq2::hisG Δpdr5::hisG Δpdr10::hisG Δpdr11::hisG Δycf1::hisG Δpdr3::hisG Δpdr15::hisG*	10
PSCDR1-GFP	AD1–8u$^-$ cells harboring CaCDR1-GFP ORF integrated at PDR5 locus	43
RPCaMDR1-GFP	AD1–8u$^-$ cells harboring CaMDR1-GFP ORF integrated at PDR5 locus	35
YGL012W Δ*erg4*	BY4742 except Δ*erg4*::*kanMX4*	Open Biosystems
YDR072C Δ*ipt1*	BY4742 except Δ*ipt1*::*kanMX4*	Open Biosystems
YML008C Δ*erg6*	BY4742 except Δ*erg6*::*kanMX4*	Open Biosystems
YNL280C Δ*erg24*	BY4742 except Δ*erg24*::*kanMX4*	Open Biosystems
YCR034W Δ*fen1*	BY4742 except Δ*fen1*::*kanMX4*	Open Biosystems
YLR372W Δ*sur4*	BY4742 except Δ*sur4*::*kanMX4*	Open Biosystems
Δ*sur4*/CaCDR1-GFP	Δ*sur4* strain expressing CaCdr1p-GFP at PDR5 locus	This study
Δ*fen1*/CaCDR1-GFP	Δ*fen1* strain expressing CaCdr1p-GFP at PDR5 locus	This study
Δ*erg6*/CaCDR1-GFP	Δ*erg6* strain expressing CaCdr1p-GFP at PDR5 locus	This study
Δ*erg24*/CaCDR1-GFP	Δ*erg24* strain expressing CaCdr1p-GFP at PDR5 locus	This study
Δ*ipt1*/CaCDR1-GFP	Δ*fen1* strain expressing CaCdr1p-GFP at PDR5 locus	This study
Δ*erg4*/CaCDR1-GFP	Δ*erg4* strain expressing CaCdr1p-GFP at PDR5 locus	This study
Δ*sur4*/CaMDR1-GFP	Δ*sur4* strain expressing CaMdr1p-GFP at PDR5 locus	This study
Δ*fen1*/CaMDR1-GFP	Δ*fen1* strain expressing CaMdr1p-GFP at PDR5 locus	This study
Δ*erg6*/CaMDR1-GFP	Δ*erg6* strain expressing CaMdr1p-GFP at PDR5 locus	This study
Δ*erg24*/CaMDR1-GFP	Δ*erg24* strain expressing CaMdr1p-GFP at PDR5 locus	This study
Δ*ipt1*/CaMDR1-GFP	Δ*ipt1* strain expressing CaMdr1p-GFP at PDR5 locus	This study
Δ*erg4*/CaMDR1-GFP	Δ*erg4* strain expressing CaMdr1p-GFP at PDR5 locus	This study

CaCdr1p in the various mutant backgrounds is mainly due to its missorting, resulting in poor localization in the PM. CaMdr1p interestingly remains unaffected by the defects in the mutant strains. Our study clearly establishes that out of the two different classes of multidrug transporters, only one (CaCdr1p) is exclusively directed to the membrane rafts for proper localization and functioning. Coupled together, it appears that membrane sphingolipid and sterols as individual components as well as their mutual interactions are critical in sorting and functioning of the ABC efflux pump protein of yeasts.

MATERIALS AND METHODS

Materials. Media chemicals were obtained from Difco (BD Biosciences) and HiMedia (Mumbai, India). The drugs cycloheximide (CYH), 4-nitroquinoline-*N*-oxide (4-NQO), methotrexate (MTX), cerulenin (CER), and Geneticin (G418) and the protease inhibitors (phenylmethylsulfonyl fluoride, leupeptin, pepstatin A, and aprotinin) and Optiprep were obtained from Sigma Chemical Co. (St. Louis, MO). Anti-GFP monoclonal antibody was purchased from BD Biosciences (Clontech, Palo Alto, CA). ^{3}H-fluconazole (FLC) was custom prepared, and ^{3}H-methotrexate (MTX) was procured from Amersham Biosciences, United Kingdom. Fluconazole was a kind gift from Ranbaxy Laboratories (New Delhi, India).

Bacterial and yeast strains and growth media. Plasmids were maintained in *Escherichia coli* DH-5α. *E. coli* was cultured in Luria-Bertani medium (Difco, BD Biosciences), to which ampicillin was added (100 μg/ml). The yeast strains used in this study are listed in Table 1. The strains (AD1-8u$^-$ [10], PSCDR1-GFP [AD1-8u$^-$ derivative expressing CaCdr1p-GFP] [43], RPCaMDR1-GFP [AD1-8u$^-$ derivative expressing CaMdr1p-GFP] [35]) and the deletion mutants expressing either CaCdr1p-GFP or CaMdr1p-GFP were grown in yeast extract-peptone-dextrose (YEPD) broth (Bio101, Vista, CA), complete synthetic medium (CSM), or in SD Ura drop-out media (0.67% yeast nitrogen base, 0.2% drop-out mix, and 2% glucose; Difco). G418-resistant yeast colonies were selected on YEPD/G418 medium or CSM/G418 medium. For agar plates, 2.5% (wt/vol) Bacto agar (Difco, BD Biosciences) was added to the medium.

Disruption of ergosterol and sphingolipid biosynthetic genes. For disruption of ergosterol biosynthesis genes, which include *ERG24* (YNL280C), *ERG6* (YML008C), and *ERG4* (YGL012W), and sphingolipid biosynthesis genes, which include *SUR4* (YLR372W), *FEN1* (YCR034W), and *IPT1* (YDR072C), the corresponding disruption cassettes (deletion mutant fused with *kanMX4*) were amplified by PCR from the yeast knockout library (the Open Biosystems Mat**a** haploid set [http://sequence-www.stanford.edu/group/yeast_deletion_project/deletions3.html]) (Fig. 1E). The oligonucleotides used for amplification are listed in Table 2. Purified PCR fragments were transformed into PSCDR1-GFP and RPCaMDR1-GFP by the lithium acetate transformation protocol (18) and selected on plates containing G418 (250 μg/ml), to obtain the strains mentioned in Table 1. The correct integration of the disruption cassette in the target gene was confirmed by PCR (data not shown). Proper expression of the protein in these lipid knockouts was also confirmed by Western blotting (discussed below).

Drug susceptibility assay. The various mutant strains were tested for their susceptibility to several drugs by spot assays. Freshly streaked cells were grown overnight suspended in normal saline to an optical density at 600 nm (OD_{600}) of 0.1 (0.1 OD corresponds to 1×10^6 cells/ml of yeast cells). Five microliters of fivefold serial dilutions of 0.1 OD of each yeast culture suspension was spotted at the following concentrations: 1:5 dilution (200,000 cells), 1:25 dilution (40,000 cells), 1:125 dilution (8,000 cells), and 1:625 dilution (1,600 cells). These were spotted onto agar plates in the absence (control) or in the presence of the drugs (35).

Drug transport. Accumulation of ^{3}H-MTX (specific activity, 8.60 Ci/mmol) and ^{3}H-FLC (specific activity, 19 Ci/mmol) was determined essentially by the protocol described previously (35). For accumulation assays, 25 μM of ^{3}H-MTX and 100 nM of ^{3}H-FLC was routinely used.

Confocal microscopy and flow cytometry. Confocal imaging and flow cytometry (fluorescence-activated cell sorter [FACS]) analysis of CaCdr1p-GFP, CaMdr1p-GFP, and lipid mutants expressing these two proteins were performed under an oil immersion objective at ×100 magnification on a confocal microscope (Radiance 2100, AGR, 3Q/BLD; Bio-Rad, United Kingdom) and a FACSort flow cytometer (Becton-Dickson Immunocytometry Systems, San Jose, CA) as described previously (43).

Immunodetection of CaCdr1p and CaMdr1p. Purified PM fractions of yeast cells were prepared as described previously (43). The PM protein concentration was determined by bicinchoninic acid assay using bovine serum albumin as the standard. Forty micrograms of each PM protein sample was electrophoresed by sodium dodecyl sulfate-polyacrylamide gel electrophoresis (SDS-PAGE), transferred to nitrocellulose membrane, and Western blotted using primary monoclonal α-GFP (1:5,000) (BD Biosciences) or polyclonal α-Pma1p antibody for PM-ATPase (1:1,000) antibody (provided by R. Serrano). Primary antibodies were detected with horseradish peroxidase-conjugated secondary antibody (1:5,000), followed by detection of chemiluminescence (ECL kit; Amersham) (43).

Isolation of membrane rafts. Lipid rafts were isolated according to the method of Bagnat et al. (2), with the following modification: crude membranes, instead of the whole-cell extract, were used for the detergent extraction analysis. An amount of cells equivalent to 100 OD_{600} units of an overnight culture was broken by vortexing with glass beads in TNE buffer (50 mM Tris-HCl, pH 7.4, 150 mM NaCl, 5 mM EDTA) supplemented with leupeptin (4 μM) and pepstatin (2 μM).

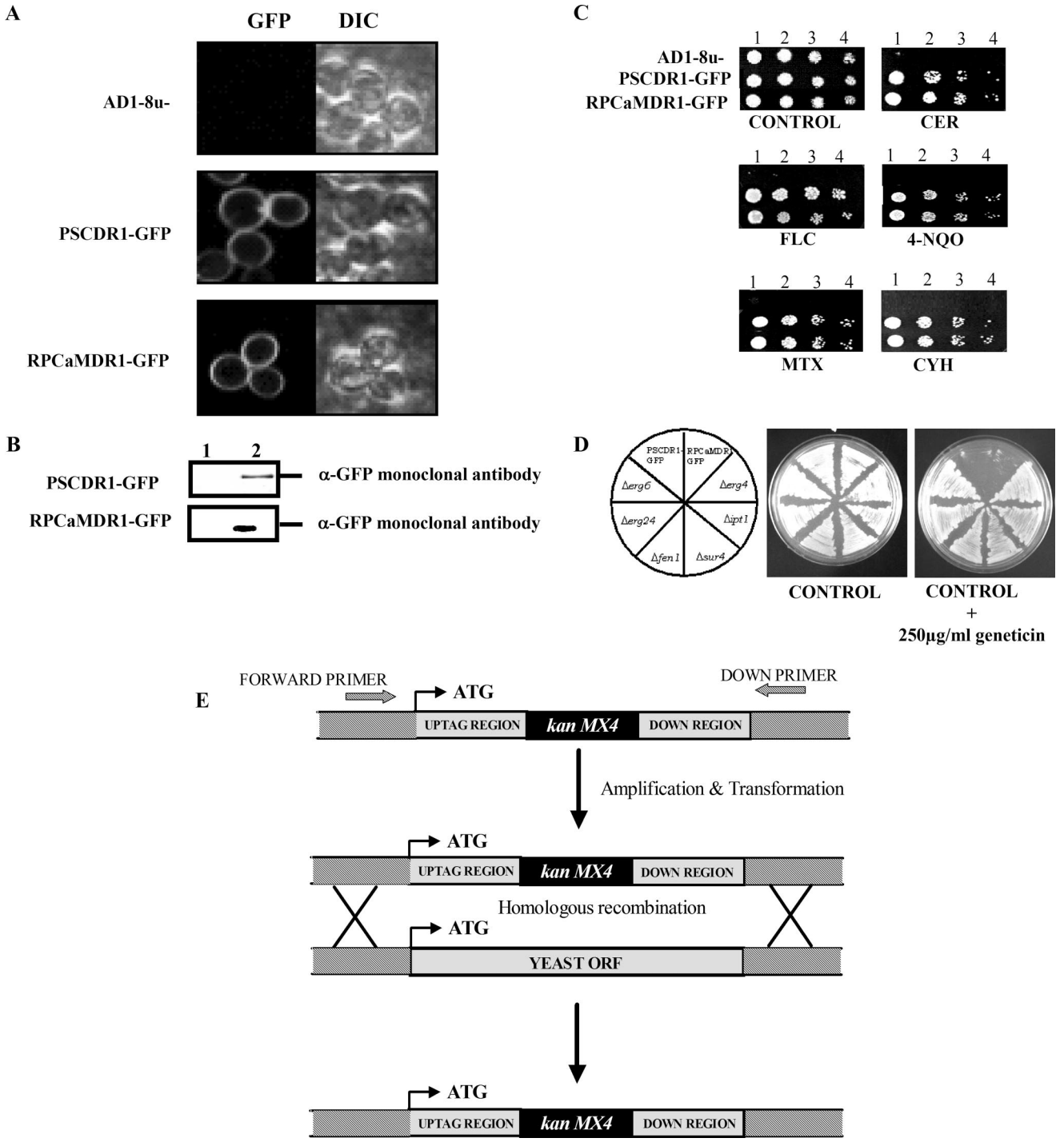

FIG. 1. (A) Differential interference contrast (DIC) (right panels) and confocal (left panels) images of the control AD1-8u$^-$, PSCDR1-GFP (AD1-8u$^-$ expressing CaCdr1p-GFP), and RPCaMDR1-GFP (AD1-8u$^-$ expressing CaMdr1p-GFP) strains. Both GFP-tagged proteins showed typical rimmed appearance on the periphery of the cells. (B) PM protein (40 μg) from each strain was loaded on the SDS-PAGE gel and electrophoresed for Western blotting. The GFP-tagged proteins in the strains AD1-8u$^-$ (control strain, lane 1 in both panels), PSCDR1-GFP (lane 2, upper panel), and RPCaMDR1-GFP (lane 2, lower panel) were detected with α-GFP primary monoclonal antibody, showing that the proteins are properly expressed and targeted. Primary antibodies were detected with horseradish peroxidase-conjugated secondary antibody, followed by detection of chemiluminescence (ECL kit; Amersham) (43). (C) Spot assays, showing the pattern of drug resistance of AD1-8u$^-$, PSCDR1-GFP, and RPCaMDR1-GFP strains. Cells were resuspended in normal saline to an OD_{600} of 0.1 (0.1 OD corresponding to 1×10^6 cells/ml). Five microliters of fivefold serial dilutions of 0.1 OD culture of each yeast strain suspension was then spotted in concentrations of 1:5 (1), 1:25 (2), 1:125 (3), and 1:625 (4) on agar plates in the absence (control) and the presence of various drugs: FLC (0.17 μg/ml), CYH (0.2 μg/ml), CER (3 μg/ml), 4-NQO (0.2 μg/ml), and MTX (65 μg/ml). Growth differences were recorded following incubation of the plates for 48 h at 30°C. (D) Plates showing sensitivity of the PSCDR1-GFP and RPCaMDR1-GFP strains for G418, which is used as the selection marker for transformation, while the lipid knockout mutants from the yeast knockout library are resistant to G418. (E) Strategy for the disruption of the genes involved: PCR amplification of the disruption cassette with homology to the region flanking the ORFs of the gene to be disrupted with G418 as the selection marker (deletion mutant fused with *kanMX4*) (5, 45), followed by integration of the amplicon by the lithium acetate transformation protocol (18).

TABLE 2. List of the oligonucleotides used in this study

Primer	Sequence	Purpose
F1AMP	5′-TGGTCCTGCTATCATGCTATTG-3′	Forward primer for amplifying Δ*erg4*::*kanMX4*
R1AMP	5′-AATGGCTAACCTTTCCCAAATC-3′	Reverse primer for amplifying Δ*erg4*::*kanMX4*
F11AMP	5′-CCTCTGATTGTGCTGATTGATTC-3′	Forward primer for amplifying Δ*ipt1*::*kanMX4*
R11AMP	5′-TCTGAAGCTCTTTCGTTTGGTG-3′	Reverse primer for amplifying Δ*ipt1*::*kanMX4*
ERG6-F	5′-CCGATAACTTCTTCATTGCTT-3′	Forward primer for amplifying Δ*erg6*::*kanMX4*
ERG6-R	5′-CTGATAGAAAATACTGGTCGT-3′	Reverse primer for amplifying Δ*erg6*::*kanMX4*
ERG24-F	5′-CATTGTGTGAAGGTTGTGCAT-3′	Forward primer for amplifying Δ*erg24*::*kanMX4*
ERG24-R	5′-AGCGTTGCATAGATAGACCAC-3′	Reverse primer for amplifying Δ*erg24*::*kanMX4*
FEN1-F	5′-GAAAATCGCAAAACCCACAG-3′	Forward primer for amplifying Δ*fen1*::*kanMX4*
FEN1-R	5′-CTAAAATAACGCCAGAAATG-3′	Reverse primer for amplifying Δ*fen1*::*kanMX4*
SUR4-F	5′-TGGAGTCTTCTGTTTGTTGTT-3′	Forward primer for amplifying Δ*sur4*::*kanMX4*
SUR4-R	5′-GGACACTTTACAAACTGCAAG-3′	Reverse primer for amplifying Δ*sur4*::*kanMX4*

After low-speed centrifugation, crude membranes were collected by centrifugation (30 min at 58,000 × *g*; Beckman Ti 70.1 rotor at 4°C). Aliquots of crude membranes (200 μg of total protein) were resuspended in 270 μl of TNE buffer. Triton X-100 was added to a final concentration of 1%, and the mixture was incubated for 30 min on ice. Then, Optiprep (Sigma) was added to a final concentration of 40% (wt/vol). The samples transferred to centrifuge tubes were overlaid with 1.32 ml of 30% Optiprep in TXNE (TNE plus 0.1% Triton X-100) followed by 220 μl of TXNE and were centrifuged for 2 h at 259,000 × *g* in a Beckman TLS55 rotor at 4°C. Six equal fractions were collected from the top of each gradient, where the proteins were precipitated with trichloroacetic acid (final concentration, 10%) and collected by centrifugation at 4°C. This step was required to prevent proteolysis by residual endogeneous proteases. The pellets were neutralized by and dissolved in 10 μl of 1 M Tris base and 25 μl of dissociation buffer (0.1 M Tris-HCl, pH 6.8, 4 mM EDTA, 4% SDS, 20% glycerol, 2% 2-mercaptoethanol, 0.02% bromphenol blue). The samples were incubated at 37°C for 15 min and analyzed by SDS-PAGE and immunoblotting as described above.

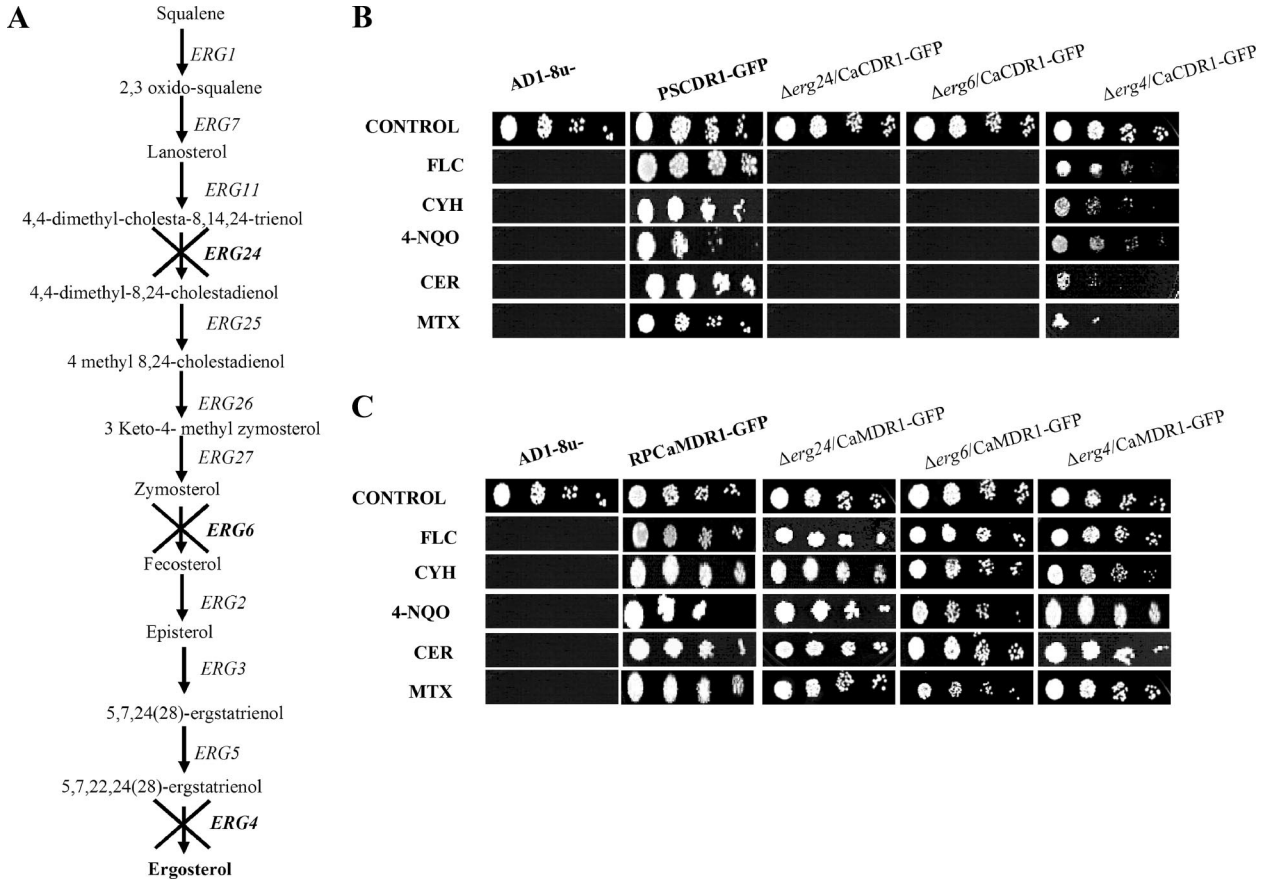

FIG. 2. (A) Schematic representation of the ergosterol biosynthetic pathway. The genes disrupted are shown with a cross in the pathway. Disrupted genes include the following: *ERG24*, *ERG6*, and *ERG4*. (B and C) Spot assays with AD1-8u$^-$, PSCDR1-GFP, RPCaMDR1-GFP, and ergosterol mutants (Δ*erg24*, Δ*erg6*, and Δ*erg4*) expressing CaCdr1p or CaMdr1p-GFP. Cells were freshly streaked and grown overnight and were resuspended in normal saline to an OD_{600} of 0.1 (0.1 OD corresponding to 1×10^6 cells/ml). Five microliters of fivefold serial dilutions of 0.1 OD culture of each yeast strain suspension was then spotted in concentrations of 1:5, 1:25, 1:125, and 1:625 on agar plates containing different drugs: FLC (0.17 μg/ml), CYH (0.2 μg/ml), CER (3 μg/ml), 4-NQO (0.2 μg/ml), and MTX (65 μg/ml). Growth differences were recorded following incubation of the plates for 48 h at 30°C.

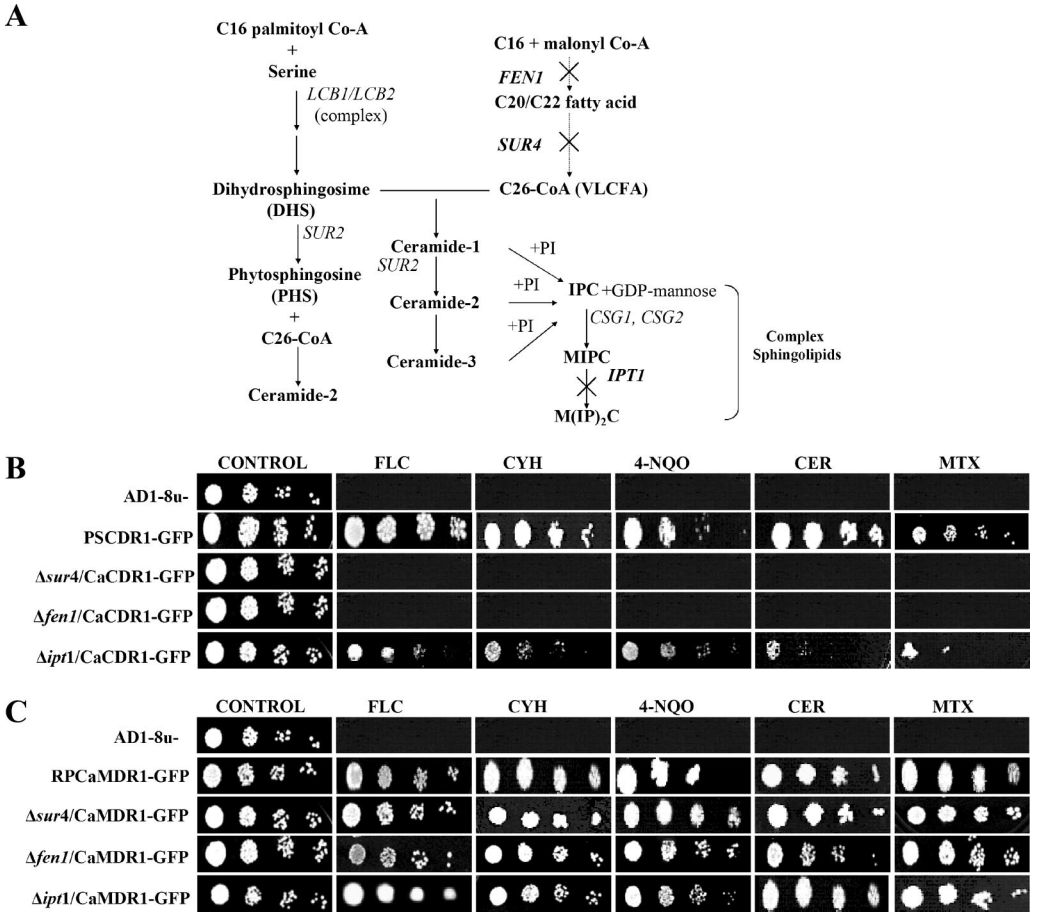

FIG. 3. (A) Schematic representation of the sphingolipid biosynthetic pathway in fungi. The disrupted genes *FEN1*, *SUR4*, and *IPT1* are shown with a cross in the pathway. (B and C) Spot assays with AD1-8u$^-$, PSCDR1-GFP, RPCaMDR1-GFP, and sphingolipid mutants (Δ*fen1*, Δ*sur4*, or Δ*ipt1*) expressing CaCdr1p-GFP or CaMdr1p-GFP. Five-microliter samples of fivefold serial dilutions of each yeast culture (each with cells suspended in normal saline to an OD_{600} of 0.1) (0.1 OD corresponding to 1×10^6 cells/ml) were spotted onto agar plates in the absence (control) or in the presence of the following drugs (35): FLC (0.17 μg/ml), CYH (0.2 μg/ml), CER (3 μg/ml), 4-NQO (0.2 μg/ml), and MTX (65 μg/ml). Growth differences were recorded following incubation of the plates for 48 h at 30°C.

RESULTS

Overexpression of GFP-tagged CaCdr1p and CaMdr1p. In this study, we exploited the well-established and extensively used expression system of *S. cerevisiae* for the overexpression of CaCdr1p and CaMdr1p (10, 25, 35, 42, 43). The strategy of GFP tagging and cloning of CaCdr1p and CaMdr1p in the plasmid pSK-PDR5PPUS was described previously (35, 43). The rimmed appearance of strains expressing GFP-tagged CaCdr1p (PSCDR1-GFP) and CaMdr1p (RPCaMDR1-GFP) under confocal microscopy and Western blot analysis of the PM fractions of the strains confirmed their proper expression and surface localization (Fig. 1A and B). Spot assays for drug susceptibility revealed that both the proteins are fully functional (Fig. 1C).

Deletion of ergosterol and sphingolipid biosynthetic genes. PSCDR1-GFP and RPCaMDR1-GFP (AD1-8u$^-$ derivatives expressing CaCdr1p and CaMdr1p, respectively) were tested for their sensitivity to the drug G418, which is the selectable marker of the 'yeast knockout' (YKO) collection of *S. cerevisiae* (Open Biosystems Mat**a** haploid set) (Fig. 1D). Both PSCDR1-GFP and RPCaMDR1-GFP strains were sensitive to G418 (Fig. 1D). The knockout was based on a PCR-generated deletion strategy, which was used to systematically replace the yeast open reading frame (ORF) from its start to stop codon with a *kanMX4* module (5, 45). The disruption cassette with homology to the region flanking the ORFs of the gene to be disrupted and with G418 as the selection marker was amplified (Fig. 1E), and the amplicon was purified and transformed by the lithium acetate transformation protocol (18). The integration of the disruption cassette at the right locus was confirmed by PCR (data not shown). The genes disrupted in the sphingolipid biosynthesis pathway in PSCDR1-GFP and RPCaMDR1-GFP included the following: *FEN1*, which codes for fatty acid elongase and acts on fatty acids of up to 24 carbons in length (Δ*fen1*/CaCDR1-GFP and Δ*fen1*/CaMDR1-GFP); *SUR4*, which also codes for an elongase, involved in fatty acid and sphingolipid biosynthesis and synthesizes very-long-chain, 20- to 26-carbon fatty acids from C-18–coenzyme A primers (Δ*sur4*/CaCDR1-GFP and Δ*sur4*/CaMDR1-GFP); and *IPT1*, which codes for inositol phosphotransferase 1, involved in synthesis of mannose-(inositol-P)$_2$-ceramide [M(IP)$_2$C] (Δ*ipt1*/CaCDR1-GFP and Δ*ipt1*/CaMDR1-GFP). In the ergosterol biosynthesis pathway, we disrupted the following genes:

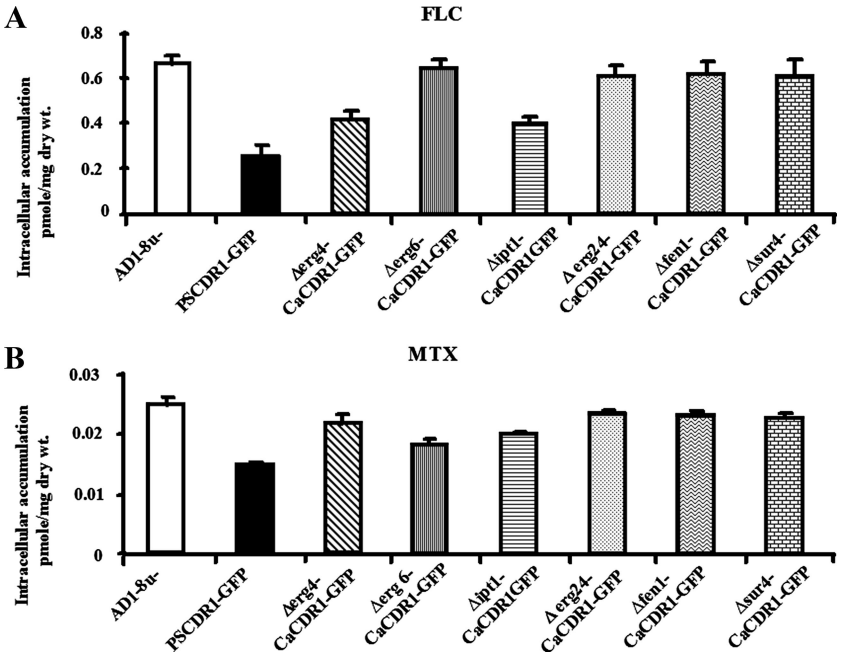

FIG. 4. ^{3}H-MTX and ^{3}H-FLC accumulation in PSCDR1-GFP and lipid mutants expressing CaCdr1p-GFP. ^{3}H-FLC (A) and ^{3}H-MTX (B) accumulation in sphingolipid mutants Δ*sur4*, Δ*fen1*, and Δ*ipt1* and ergosterol mutants Δ*erg6*, Δ*erg24*, and Δ*erg4*, expressing CaCdr1p-GFP. AD1-8u$^-$ is shown as the control. The values plotted are from 10 min after commencement of transport. The results are the means ± standard deviations of three independent experiments.

ERG24, which codes for C-14 sterol reductase (Δ*erg24*/CaCDR1-GFP and Δ*erg24*/CaMDR1-GFP); *ERG6*, which codes for Δ(24)-sterol C-methyltransferase (Δ*erg6*/CaCDR1-GFP and Δ*erg6*/CaMDR1-GFP); and *ERG4*, which encodes for sterol C-24(28) reductase (Δ*erg4*/CaCDR1-GFP and Δ*erg4*/CaMDR1-GFP) (Table 1). The respective positions of all these genes in the ergosterol and sphingolipid biosynthetic pathways are shown in Fig. 2A and 3A, respectively.

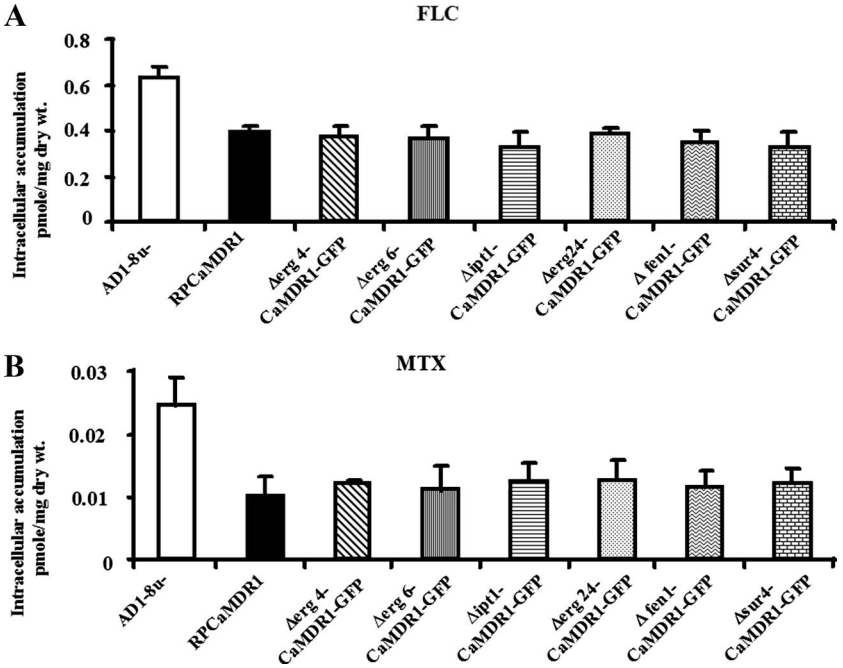

FIG. 5. ^{3}H-MTX and ^{3}H-FLC accumulation in RPCaMDR1-GFP and lipid mutants expressing CaMdr1p-GFP. Accumulation of ^{3}H-FLC (A) and ^{3}H-MTX (B) for sphingolipid mutants Δ*sur4*, Δ*fen1*, and Δ*ipt1* and ergosterol mutants Δ*erg6*, Δ*erg24*, and Δ*erg4*, expressing CaMdr1p-GFP. The values plotted are from 10 min after commencement of transport. The results are the means ± standard deviations of three independent experiments.

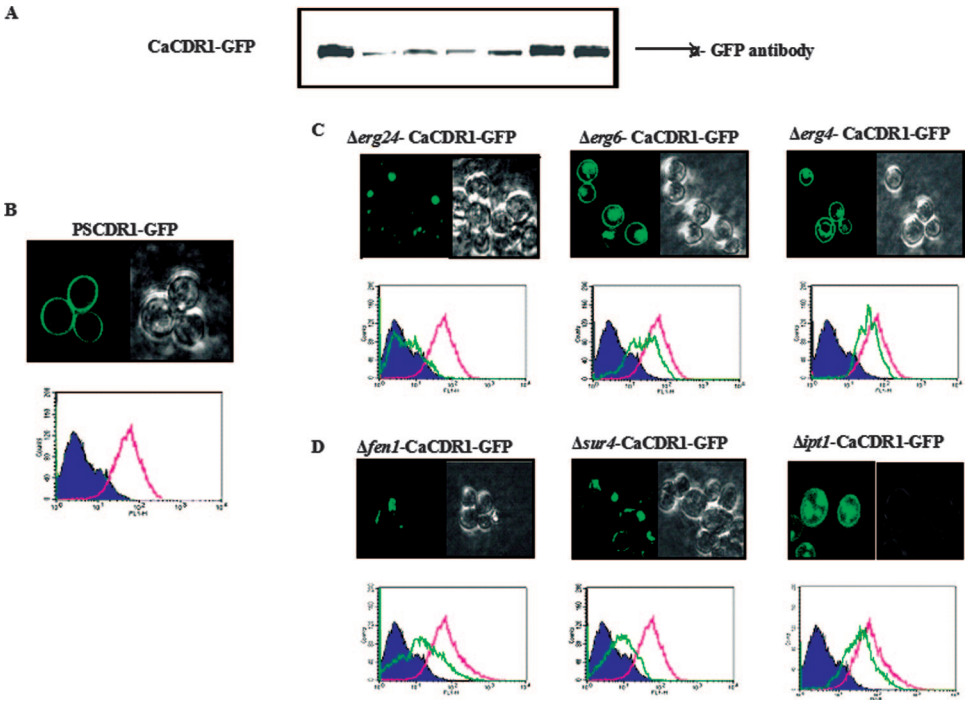

FIG. 6. (A) Immunodetection of CaCdr1p in the PM of strain PSCDR1-GFP and lipid mutants expressing CaCdr1p-GFP. PM protein (40 μg) from each strain was electrophoresed on SDS-PAGE, transferred to nitrocellulose, and Western blotted. The presence of the GFP-tagged CaCdr1p was detected by immunoblotting with α-GFP monoclonal primary antibody and detected with horseradish peroxidase-conjugated secondary antibody, followed by detection of chemiluminescence (ECL kit; Amersham) (43). WT, wild type. (B) Fluorescence imaging (upper panel) by confocal microscopy shows membrane localization of CaCdr1p-GFP. Flow cytometry (lower panel) of *S. cerevisiae* expressing CaCdr1p-GFP and lipid mutants expressing GFP-tagged Ca*CDR1*. The histogram derived from the Cell Quest program depicts the total fluorescence intensities of AD1-8u$^-$ (control) (purple filled area) and PSCDR1-GFP (solid pink line) for each panel, and the other extra line (solid green) represents those of the respective lipid mutant variants expressing CaCdr1p-GFP.

CaCdr1p-mediated drug resistance depends on the membrane lipid status. To analyze the activity of CaCdr1p-GFP- and CaMdr1p-GFP-expressing strains in the ergosterol and sphingolipid biosynthetic mutant backgrounds, the strains were tested for their susceptibility to different drug substrates by spot assays. In comparison to the highly sensitive AD1-8u$^-$ cells (Fig. 1C), which showed almost no growth in the presence of the drugs, cells expressing wild-type CaCdr1p-GFP (PSCDR1-GFP) (43) and CaMdr1p-GFP (RPCaMDR1-GFP) (35) were able to tolerate the same concentrations of all the tested drugs, such as FLC, CYH, MTX, 4-NQO, and CER. Thus, all the tested drugs are substrates of CaCdr1p as well as of CaMdr1p. We had previously observed that although both FLC and MTX can be transported by CaCdr1p and CaMdr1p, the former is a better substrate of CaCdr1p while the latter is a preferred substrate of CaMdr1p (35).

Overexpression of CaCdr1p-GFP in ergosterol (Δ*erg24*/CaCDR1-GFP, Δ*erg6*/CaCDR1-GFP, and Δ*erg4*/CaCDR1-GFP) (Fig. 2B) or sphingolipid (Δ*sur4*/CaCDR1-GFP, Δ*fen1*/CaCDR1-GFP, and Δ*ipt1*/CaCDR1-GFP) (Fig. 3B) knockout strains resulted in hypersensitivity to drugs. In contrast, no abrogation of drug resistance was observed in CaMdr1p-GFP when expressed in the above null mutants (Fig. 2C and 3C). These results were also confirmed by the microdilution method (data not shown).

Notably, Δ*erg4* and Δ*ipt1* mutants expressing CaCdr1p were relatively less sensitive to all the tested drugs than were the other knockout mutants. Both *ERG4* and *IPT1* catalyze the last step in the ergosterol and sphingolipid biosynthesis pathways, respectively, and the absence of these in Δ*ipt1* and Δ*erg4* cells selectively prevents the formation of the end product, though the precursors of the pathway are still present. These precursors are probably able to compensate for the absence of ergosterol or $M(IP)_2C$ on the membrane. Additionally, both CaCdr1p and CaMdr1p proteins, as revealed by Western blotting and confocal images, are not totally mislocalized in Δ*ipt1* and Δ*erg4* cells, which again could contribute to the observed resistance to all the drugs.

The efflux of MTX and FLC mediated by CaCdr1p-GFP was severely hampered in lipid mutants. In order to correlate CaCdr1p-GFP-mediated drug sensitivity to the reduced efflux of drugs in the ergosterol and sphingolipid mutant backgrounds, accumulation of two radiolabeled drug substrates such as ^{3}H-MTX and ^{3}H-FLC was measured. An increase or decrease in the level of accumulation of the drug, at a given time point, implies its reduced or enhanced efflux, respectively. It is apparent from Fig. 4 and 5 that, compared to the host (AD1-8u$^-$) cells, the accumulation of ^{3}H-MTX and ^{3}H-FLC was considerably reduced (more efflux) in cells expressing CaCdr1p-GFP- and CaMdr1p-GFP-tagged proteins. We examined the efflux activity of CaCdr1p-GFP in the lipid null mutant backgrounds by measuring the accumulation of drug substrates in cells expressing CaCdr1p-GFP, namely, Δ*sur4*/CaCDR1-GFP, Δ*fen1*/CaCDR1-GFP, Δ*erg6*/CaCDR1-GFP,

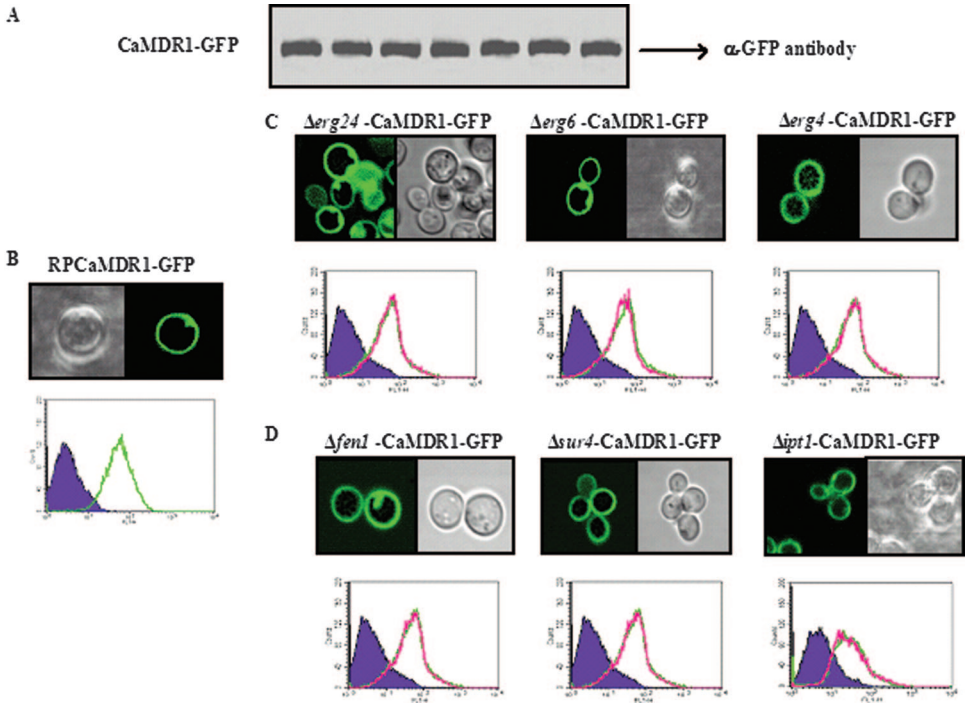

FIG. 7. (A) Immunodetection of CaMdr1p in the PM of strain RPCaMDR1-GFP and lipid mutants expressing CaMdr1p-GFP. PM protein samples (40 μg) from each strain were electrophoresed through SDS-PAGE and analyzed by Western blotting with α-GFP monoclonal primary antibody. Primary antibodies were detected with horseradish peroxidase-conjugated secondary antibody, followed by detection of chemiluminescence (ECL kit; Amersham) (43). WT, wild type. (B) Fluorescence imaging (upper panel) by confocal microscopy showing membrane localization of CaMdr1p-GFP. Flow cytometry (lower panel) of *S. cerevisiae* expressing CaMdr1p-GFP and lipid mutants expressing GFP-tagged Ca*MDR1*. The histogram derived from the Cell Quest program depicts the total fluorescence intensities of AD1-8u$^-$ (control) (purple filled area) and RPCaMDR1-GFP (solid green line) for each panel, and the other extra line (solid pink) represents those of the respective lipid mutant variants expressing CaMdr1p-GFP.

Δ*erg24*/CaCDR1-GFP, Δ*ipt1*/CaCDR1-GFP, and Δ*erg4*/CaCDR1-GFP. The accumulation was significantly increased (decrease in efflux) for FLC (between 24 and 57%) and for MTX (between 13 and 35%), compared with the accumulation of these drugs in normal cells expressing CaCdr1p-GFP (Fig. 4A and B). In comparison, CaMdr1p-GFP, when expressed in the same backgrounds, showed no significant difference in its ability to efflux both the drugs (Fig. 5A and B). In general, the accumulation data matched well with the level of sensitivity observed for the drugs. For example, among ergosterol mutants, Δ*erg24* and Δ*erg6* are more sensitive to drugs than Δ*erg4* cells, and this difference is also reflected in the accumulation of FLC and MTX, wherein sensitive Δ*erg24* and Δ*erg6* strains accumulate much higher levels (reduced efflux) of drug than the less-sensitive Δ*erg4* mutant cells. This is also true for Δ*ipt1* versus Δ*fen1* and Δ*sur4*. The sensitive Δ*fen1* and Δ*sur4* show much higher accumulation of the drug than the Δ*ipt1* cells.

Lipid imbalance caused selective recruitment defect of CaCdr1p-GFP. We also examined the effect of lipid changes on CaCdr1p-GFP localization in the PM. Immunoblot results demonstrated that between CaMdr1p and CaCdr1p (Fig. 6 and Fig. 7), the expression of the latter in the PM was considerably reduced in most of the ergosterol (Δ*erg6*/CaCDR1-GFP, Δ*erg24*/CaCDR1-GFP, and Δ*erg4*/CaCDR1-GFP) and sphingolipid (Δ*sur4*/CaCDR1-GFP, Δ*fen1*/CaCDR1-GFP, and Δ*ipt1*/CaCDR1-GFP) null mutants compared to that in control cells expressing CaCdr1p-GFP (Fig. 6A). Confocal images of CaCdr1p-GFP in the null mutants also showed poor surface localization, as was evident from the lack of total rimmed appearance on the periphery of the cells and trapped GFP fluorescence inside the cells (Fig. 6B, C, and D, upper panels). Results obtained from FACS analyses also showed reduced total fluorescence, which was consistent with the immunoblot and confocal data confirming poor expression of CaCdr1p in the PM (Fig. 6C and D, lower panels). Interestingly, the characteristic distribution of CaCdr1p in DRMs was lost in all the lipid mutants (Fig. 8D). However, in the Δ*erg6* mutant, similar to the control strain (top panel), CaCdr1p protein is visible in fractions 1 and 2, but unlike the control strain, a majority of CaCdr1p was present in fractions 5 and 6. Thus, mislocalization of CaCdr1p in Δ*erg6* did not appear to be complete, as was the case with other mutants. Notwithstanding this, Δ*erg6* mutation was sufficient to result in mislocalization of a majority of CaCdr1p.

CaCdr1p is localized in membrane rafts. Ergosterol and sphingolipids are major constituents of lipid rafts, also called DRMs for their property of being resistant to solubilization when treated with nonionic detergents at low temperature (1, 2, 15, 22). Since we observed that CaCdr1p is mislocalized following imbalances in raft lipid constituents, we checked if CaCdr1p is associated with these discrete DRMs. For this, we isolated membrane rafts by the detergent insolubility method using the nonionic detergent Triton X-100 (2, 12, 21, 28, 31) as described in Materials and Methods. We used Optiprep for

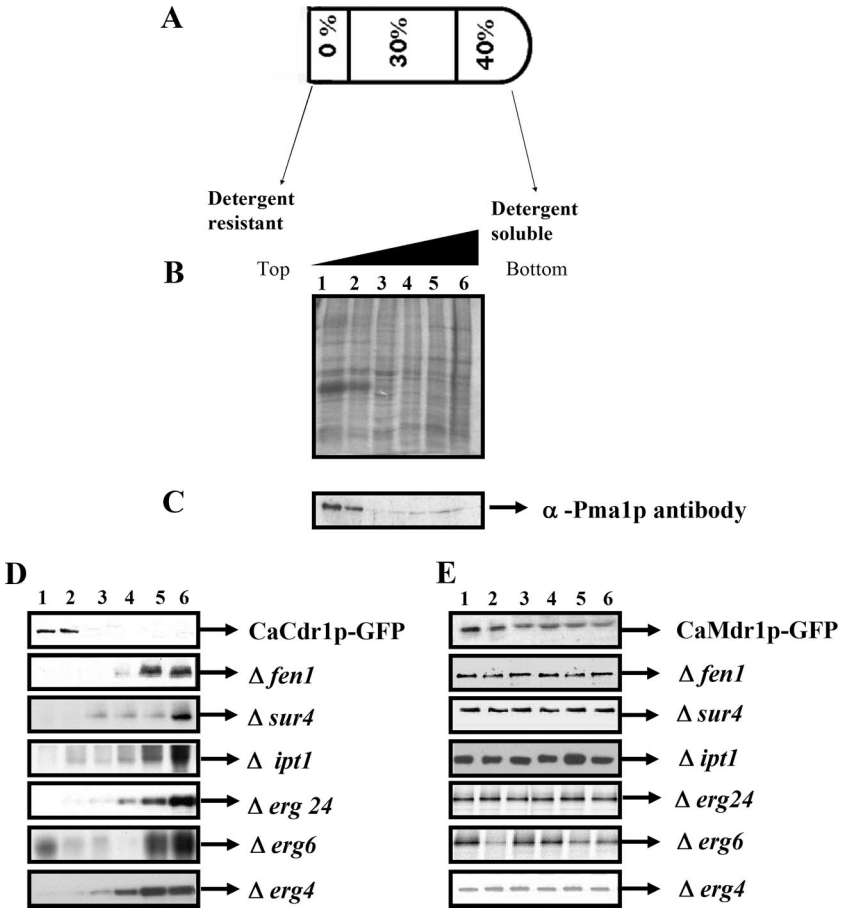

FIG. 8. Isolation of DRMs from yeast. (A) Schematic of the gradient, illustrating the concentration of Optiprep in each step. (B) Proteins isolated from six gradient fractions, separated by SDS-PAGE. (C) Immunoblot of Pma1p with α-Pma1p primary polyclonal antibody which was detected with horseradish peroxidase-conjugated secondary antibody, followed by detection of chemiluminescence (ECL kit; Amersham) (43) to confirm raft preparation. (D) Immunoblot of gradient fractions of CaCdr1p with α-GFP monoclonal primary antibody in the wild-type (WT) (upper panel), detected with horseradish peroxidase-conjugated secondary antibody in sphingolipid mutants Δ*sur4*, Δ*fen1*, and Δ*ipt1* and ergosterol mutants Δ*erg6*, Δ*erg24*, or Δ*erg4* expressing CaCdr1p-GFP. (E) Immunoblot of gradient fractions of CaMdr1p with α-GFP monoclonal antibody in the wild type (upper panel), sphingolipid mutants Δ*sur4*, Δ*fen1*, and Δ*ipt1*, and ergosterol mutants Δ*erg6*, Δ*erg24*, and Δ*erg4* expressing CaMdr1p-GFP.

gradient formations wherein DRM generally constitutes the upper two fractions, when six equal fractions from top to bottom are taken (12, 21, 28) (Fig. 8A). Immunoblot analysis with monoclonal α-GFP primary antibody of the DRM fractions clearly showed the presence of CaCdr1p in the top two floating raft fractions (Fig. 8D, first panel). The raft preparation was verified by reprobing the immunoblot with the polyclonal α-Pma1p secondary antibody (Fig. 8C), which is a positive marker for raft proteins (1, 2, 19). The MFS transporter CaMdr1p, on the other hand, was not exclusively present in raft fractions but rather was evenly distributed in all the fractions. This distribution pattern of CaMdr1p remained unaffected by the lipid perturbations (Fig. 8E).

DISCUSSION

Our results show that the cells expressing the ABC transporter CaCdr1p in lipid mutants (either defective in sphingolipid or ergosterol biosynthesis) turned sensitive to the tested drugs, which was also evident from their abrogated efflux of drug substrates. In comparison, cells expressing the MFS transporter CaMdr1p in the same lipid mutant background remained properly surface localized, displayed resistance to drugs, and showed unaltered efflux of drug substrates. Taken together, both ergosterol and sphingolipids, being principle constituents of membrane lateral microdomains, were found to be important for CaCdr1p localization. Since the disruption of ergosterol and sphingolipid biosynthetic genes lead to mislocalization of CaCdr1p, it should be noted that the observed poor efflux of drugs mediated by CaCdr1p and the enhanced drug sensitivity of null mutants were mainly due to this mislocalization instead of its impaired functioning.

A recent proteomic analysis of DRMs from *C. albicans* identified 29 proteins to be localized within membrane rafts (22). In that study, CaCdr1p was not detected in DRMs, which could have been due to the poor level of expression of CaCdr1p in the laboratory isolate SC5314. Some other known raft proteins including amino acid permease Fur4p, Tat2p, and transporters Can1p and Nce2p were also not detected in that study (22).

The expression of the protein in a heterologous background probably does not affect its association with the raft, as Hup1p of *Chlorella kessleri*, which exclusively exists in rafts, when expressed in *S. cerevisiae*, still retained its property of being localized within the DRM microdomains (20). Interestingly, only certain proteins are localized within DRMs. Yeast PM-ATPase is one such example, which is exclusively found within rafts. The oligomerization of Pma1p has been linked to membrane lipid composition, since in ceramide-depleted cells, Pma1p remains monomeric (27). Our present study also confirms that, similar to CaCdr1p, the PM-ATPase protein is localized within rafts and is mistargeted in lipid mutant backgrounds (data not shown). Although, it would seem logical to predict the localization of proton-generating (Pma1p) and -utilizing (CaMdr1p) proteins within the same membrane lateral domains, our study demonstrates that this is not the case and apparently tight coupling between proton motive force-generating Pma1p and proton motive force-dissipating CaMdr1p is not obligatory.

The association of certain proteins with a raft has emerged as an important regulator of signal transduction, protein- and membrane-polarized intracellular sorting, cytoskeletal reorganization, and entry of infectious organisms in living cells (23). In *C. albicans*, glycosylphosphatidylinositol-anchored proteins Eap1p, Dfg5p, and Phr1p are present in DRMs and are known to be involved in adhesion to epithelial cells, virulence, and proper hyphal growth (29). Gas1p from *S. cerevisiae* is involved in cell wall biogenesis and is a known lipid raft protein (1, 3, 29). The functional significance of the PM compartmentalization is evident by the protein distribution in polarized, mating-induced *Schizosaccharomyces pombe* cells and in *S. cerevisiae*, which harbors proteins in the shmoo that are required for mating (3, 46). The hyphal tips of *C. albicans* also show ergosterol-enriched domains, which may be indicative of clustering of DRMs in its growing tip (29). We had previously observed that Ca*CDR1* is highly expressed during hyphal development in *C. albicans* cells (14). With this background, it is tempting to speculate that if CaCdr1p is also localized on growing hyphal tips then it may have a role in the morphogenesis of *Candida* as well. It may not be out of context to mention that most of the transcription factors regulating *C. albicans* morphogenesis also regulate Ca*CDR1* (33). In this context, the role of rafts as a hub of signaling in *Candida* cells remains to be examined.

ACKNOWLEDGMENTS

We thank R. D. Cannon and K. Natarjan for providing us with the plasmids and strains. We also thank R. Serrano for the PM-ATPase antibodies and Ranbaxy Laboratories Limited, India, for providing fluconazole.

The work presented in this paper has been supported in part by grants (to R. Prasad) from the Department of Biotechnology [DBT/PR3825/Med/14/488(a)/2003], Council of Scientific and Industrial Research [38(1122)/06/EMR-II)], and Department of Science and Technology (SR/SO/BB-12/2004), India. S.L.P. acknowledges a grant from the Department of Science and Technology (SR/FT/L-26/2006), India. R. Pasrija acknowledges the Council of Scientific and Industrial Research, India, for a senior research fellowship award.

We thank Shaheed Jameel, Charu Tanwar, and Pankaj Pandotra and for their help with the confocal pictures and FACS analyses.

REFERENCES

1. **Bagnat, M., A. Chang, and K. Simons.** 2001. Plasma membrane proton ATPase Pma1p requires raft association for surface delivery in yeast. Mol. Biol. Cell **12:**4129–4138.
2. **Bagnat, M., S. Keranen, A. Shevchenko, A. Shevchenko, and K. Simons.** 2000. Lipid rafts function in biosynthetic delivery of proteins to the cell surface in yeast. Proc. Natl. Acad. Sci. USA **97:**3254–3259.
3. **Bagnat, M., and K. Simons.** 2002. Cell surface polarization during yeast mating. Proc. Natl. Acad. Sci. USA **99:**14183–14188.
4. **Balzi, E., and A. Goffeau.** 1995. Yeast multidrug resistance: the PDR network. J. Bioenerg. Biomembr. **27:**71–76.
5. **Baudin, A., O. Ozier-Kalogeropoulos, A. Denouel, A. Lacroute, and C. Cullin.** 1993. A simple and efficient method for direct gene deletion in *Saccharomyces cerevisiae*. Nucleic Acids Res. **21:**3329–3330.
6. **Braun, B. R., M. van het Hoog, C. d'Enfert, M. Martchenko, J. Dungan, A. Kuo, D. O. Inglis, M. A. Uhl, H. Hogues, M. Berriman, M. Lorenz, A. Levitin, U. Oberholzer, C. Bachewich, D. Harcus, A. Marcil, D. Dignard, T. Iouk, R. Zito, L. Frangeul, F. Tekaia, K. Rutherford, E. Wang, C. A. Munro, S. Bates, N. A. Gow, L. L. Hoyer, G. Kohler, J. Morschhauser, G. Newport, S. Znaidi, M. Raymond, B. Turcotte, G. Sherlock, M. Costanzo, J. Ihmels, J. Berman, D. Sanglard, N. Agabian, A. P. Mitchell, A. D. Johnson, M. Whiteway, and A. Nantel.** 2005. A human-curated annotation of the *Candida albicans* genome. PLoS Genet. **1:**36–57.
7. **Broco, N., S. Tenreiro, C. A. Viegas, and I. Sa-Correja.** 1999. *FLR1* gene (ORFYBR008c) is required for benomyl and methotrexate resistance in *Saccharomyces cerevisiae* and its benomyl induced expression is dependent on *Pdr3* transcriptional regulator. Yeast **15:**1595–1608.
8. **Cannon, R. D., E. Lamping, A. R. Holmes, K. Niimi, K. Tanabe, M. Niimi, and B. C. Monk.** 2007. *Candida albicans* drug resistance another way to cope with stress. Microbiology **153:**3211–3217.
9. **Decottignies, A., and A. Goffeau.** 1997. Complete inventory of the yeast ABC proteins. Nat. Genet. **15:**137–145.
10. **Decottignies, A., A. M. Grant, J. W. Nichols, H. De Wet, D. B. McIntosh, and A. Goffeau.** 1998. ATPase and multidrug transport activities of the overexpressed yeast ABC protein Yor1p. J. Biol. Chem. **273:**12612–12622.
11. **Demeule, M., J. Jodoin, D. Gingras, and R. Beliveau.** 2000. P-glycoprotein is localized in caveolae in resistant cells and in brain capillaries. FEBS Lett. **466:**219–224.
12. **Denny, P. W., M. C. Field, and D. F. Smith.** 2001. GPI-anchored proteins and glycoconjugates segregate into lipid rafts in Kinetoplastida. FEBS Lett. **491:**148–153.
13. **Dieterich, C., M. Schander, M. Noll, F.-J. Johannes, H. Brunner, T. Graeve, and S. Rupp.** 2002. In vitro reconstructed human epithelia reveal contributions of *Candida albicans EFG1* and *CPH1* to adhesion and invasion. Microbiology **148:**497–506.
14. **Dogra, S., S. Krishnamurthy, V. Gupta, B. L. Dixit, C. M. Gupta, D. Sanglard, and R. Prasad.** 1999. Asymmetric distribution of phosphatidylethanolamine in *C. albicans*: possible mediation by *CDR1*, a multidrug transporter belonging to ATP binding cassette (ABC) superfamily. Yeast **15:**111–121.
15. **Eric, K., D. G. Henrick, and P. L. Michael.** 1996. Identification of Triton X-100 insoluble membrane domains in the yeast *Saccharomyces cerevisiae*. J. Biol. Chem. **271:**32975–32980.
16. **Garrigues, A., A. E. Escargueil, and S. Orlowski.** 2002. The multidrug transporter, P-glycoprotein, actively mediates cholesterol redistribution in the cell membrane. Proc. Natl. Acad. Sci. USA **99:**10347–10352.
17. **Gaur, M., D. Choudhury, and R. Prasad.** 2005. Complete inventory of ABC proteins in human pathogenic yeast, Candida albicans. J. Mol. Microbiol. Biotechnol. **9:**3–15.
18. **Geitz, R. D., R. H. Schiestl, A. R. Willems, and R. A. Woods.** 1995. Studies on the transformation of intact yeast cells by the LiAc/SS-DNA/PEG procedure. Yeast **11:**355–360.
19. **Gong, X., and A. Chang.** 2001. A mutant plasma membrane ATPase, Pma1-10, is defective in stability at the yeast cell surface. Proc. Natl. Acad. Sci. USA **98:**9104–9109.
20. **Grossman, G., M. Opekarova, L. Novakova, J. Stolz, and W. Tanner.** 2006. Lipid raft-based membrane compartmentation of a plant transporter protein expressed in *S. cerevisiae*. Eukaryot. Cell **5:**945–953.
21. **Hearn, J. D., R. L. Lester, and R. C. Dickson.** 2003. The uracil transporter Fur4p associates with lipid rafts. J. Biol. Chem. **278:**3679–3686.
22. **Insenser, M. C., C. Nombela, G. Molero, and C. Gil.** 2006. Proteomic analysis of detergent-resistant membranes from *Candida albicans*. Proteomics **6:**74–81.
23. **Johanne, M., C. Stephane, M. Sebastien, F. Fabienne, F. Jerom, B. Jean-Jacques, B. Jean-Pierre, and S. P. Francoise.** 2006. Proteomics of plant detergent-resistant membranes. Mol. Cell. Proteomics **5:**1411.
24. **Kohli, A. K., M. Smriti, K. Mukhopadhyay, and R. Prasad.** 2002. In vitro low-level resistance to azoles in *Candida albicans* is associated with changes in membrane lipid fluidity and asymmetry. Antimicrob. Agents Chemother. **46:**1046–1052.
25. **Lamping, E., B. C. Monk, K. Nimmi, A. R. Holmes, S. Tsao, K. Tanabe, M. Nimmi, Y. Uehara, and R. D. Cannon.** 2007. Characterization of three

classes of membrane proteins involved in fungal azole resistance by functional hyperexpression in *Saccharomyces cerevisiae*. Eukaryot. Cell **6:**1150–1165.
26. **Lavie, Y., and M. Liscovitch.** 2001. Changes in lipid and protein constituents of rafts and caveolae in multidrug resistance cancer cells and their functional consequences. Glycoconj. J. **17:**253–259.
27. **Lee, M. C. S., S. Hamamoto, and R. Schekman.** 2002. Ceramide biosynthesis is required for the formation of the oligomeric H+-ATPase Pma1p in the yeast endoplasmic reticulum. J. Biol. Chem. **277:**22395–22401.
28. **Malinska, K., J. Malinsky, M. Opekarova, and W. Tanner.** 2003. Visualization of protein compartmentation within the plasma membrane of living yeast cells. Mol. Biol. Cell **14:**4427–4436.
29. **Martin, S. W., and J. B. Konopka.** 2004. Lipid raft polarization contributes to hyphal growth in *Candida albicans*. Eukaryot. Cell **3:**675–684.
30. **Moffett, S., D. A. Brugger, and M. E. Linder.** 2000. Lipid-dependent targeting of G proteins into rafts. J. Biol. Chem. **275:**2191–2198.
31. **Mongrand, S., J. Morel, J. Laroche, S. Claverol, J. P. Carde, M. A. Hartmann, M. Bonneu, F. Simon-Plas, R. Lessire, and J. J. Bessoule.** 2004. Lipid rafts in higher plant cells: purification and characterization of Triton X-100-insoluble microdomains from tobacco plasma membrane. J. Biol. Chem. **279:**36277–36286.
32. **Mukhopadhyay, K., T. Prasad, P. Saini, T. J. Pucadyil, A. Chattopadhyay, and R. Prasad.** 2004. Membrane sphingolipid-ergosterol interactions are important determinants of multidrug resistance in *Candida albicans*. Antimicrob. Agents Chemother. **48:**1778–1787.
33. **Murad, A. M., C. d'Enfert, C. Gaillardin, H. Tournu, F. Tekaia, D. Talibi, D. Marechal, V. Marchais, J. Cottin, and A. J. Brown.** 2001. Transcript profiling in *Candida albicans* reveals new cellular functions for the transcriptional repressors CaTup1, CaMig1 and CaNrg1. Mol. Microbiol. **42:**981–993.
34. **Pasrija, R., S. Krishnamurthy, T. Prasad, J. F. Ernst, and R. Prasad.** 2005. Squalene epoxidase encoded by *ERG1* affects morphogenesis and drug susceptibilities of *Candida albicans*. J. Antimicrob. Chemother. **55:**905–913.
35. **Pasrija, R., D. Banerjee, and R. Prasad.** 2007. Structure and function analysis of CaMdr1p, a MFS antifungal efflux transporter protein of *Candida albicans*: identification of amino acid residues critical for drug/H^+ transport. Eukaryot. Cell **6:**443–453.
36. **Pike, L. J., X. Han, and R. W. Gross.** 2005. Epidermal growth factor receptors are localized to lipid rafts that contain a balance of inner and outer leaflet lipids. J. Biol. Chem. **280:**26796–26804.
37. **Prasad, T., P. Saini, N. A. Gaur, R. A. Vishwakarma, L. A. Khan, Q. M. Haq, and R. Prasad.** 2005. Functional analysis of Ca*IPT1*, a sphingolipid biosynthetic gene involved in multidrug resistance and morphogenesis of *Candida albicans*. Antimicrob. Agents Chemother. **49:**3442–3452.
38. **Pumbwe, L., D. Glass, and H. M. Wexler.** 2006. Efflux pump overexpression in multiple-antibiotic-resistant mutants of *Bacteroides fragilis*. Antimicrob. Agents Chemother. **50:**3150–3153.
39. **Sanglard, D., F. Ischer, D. Calabrese, M. de Micheli, and J. Bille.** 1998. Multiple resistance mechanism to azole antifungals in yeast clinical isolates. Drug Resist. Updates **1:**255–265.
40. **Sanglard, D., and F. C. Odds.** 2002. Resistance of *Candida* species to antifungal agents: molecular mechanisms and clinical consequences. Lancet Infect. Dis. **2:**73–85.
41. **Schinkel, A. H., and P. Borst.** 1991. Multidrug resistance mediated by P-glycoproteins. Semin. Cancer Biol. **2:**213–226.
42. **Shukla, S., V. Rai, D. Banerjee, and R. Prasad.** 2006. Characterization of Cdr1p, a major multidrug efflux protein of *Candida albicans*: purified protein is amenable to intrinsic fluorescence analysis. Biochemistry **45:**2425–2435.
43. **Shukla, S., P. Saini, Smriti, S. Jha, S. V. Ambudkar, and R. Prasad.** 2003. Functional characterization of *Candida albicans* ABC transporter Cdr1p. Eukaryot. Cell **2:**1361–1375.
44. **Smriti, S. Krishnamurthy, and R. Prasad.** 1999. Membrane fluidity affects functions of Cdr1p, a multidrug ABC transporter of *Candida albicans*. FEMS Microbiol. Lett. **173:**475–481.
45. **Wach, A., A. Brachat, R. Pöhlmann, and P. Philippsen.** 1994. New heterologous modules for classical or PCR-based gene disruptions in *Saccharomyces cerevisiae*. Yeast **10:**1808.
46. **Wachtler, V., S. Rajagopalan, and M. K. Balasubramanian.** 2003. Sterol-rich plasma membrane domains in the fission yeast *Schizosaccharomyces pombe*. J. Cell Sci. **116:**867–874.
47. **Wu, M., D. Holowka, H. G. Craighead, and B. Baird.** 2004. Visualization of plasma membrane compartmentalization with patterned lipid bilayers. Proc. Natl. Acad. Sci. USA **101:**13798–13803.
48. **Zgurskaya, H. I.** 2002. Molecular analysis of efflux pump-based antibiotic resistance. Int. J. Med. Microbiol. **292:**95–105.